Electronic Supplementary Material (ESI) for Journal of Materials Chemistry

Supporting Information for:

Low-dimensional nanostructures fabricated from bis(dioxaborine)carbazole derivatives as fluorescent chemosensors for detecting organic amine vapors

Xingliang Liu, Xiaofei Zhang, Ran Lu,* Pengchong Xue, Defang Xu, Huipeng Zhou

State Key Laboratory of Supramolecular Structure and Materials, College of Chemistry, Jilin University, Changchun 130012, P. R. China

Fax: +86-431-88923907; *E-Mail:* luran@mail.jlu.edu.cn

Table S1. Photophysical data of **BDOBC16** in different solvents.

Solvents	λ_{abs} (nm)	λ_{em} (nm)	$\Delta\nu_{st}$ [a] /cm^{-1}
Cyclohexane	295, 332, 402, 397, 488	511	922
Toluene	296, 333, 401, 463, 501	547	1679
Benzene	295, 335, 403, 466, 504	552	1725
Diethyl ether	295, 330, 395, 457, 496	555	2143
1,4-dioxane	295, 333, 404, 465, 504	572	2359
THF	296, 333, 402, 466, 504	592	2949
Ethyl acetate	295, 332, 399 459, 500	589	3022
Chloroform	296, 334, 404, 479, 512	598	2808
DCM	295, 335, 404, 476, 513	625	3493

a. $\Delta\nu_{st} = \nu_{abs} - \nu_{em}$.

Table S2: Gelation properties of **BDOBC16** in selected organic solvents.

Solvent	BDOBC16 [a]	CGC [b] [mM]
Hexane	**I**	
Cyclohexane	**I**	
Heptane	**I**	
Benzene	**S**	
Toluene	**S**	
Xylene	**S**	
Benzene/Hexane (v/v = 1/1)	**G**	0.6
Benzene/Cyclohexane (v/v = 1/1)	**G**	0.8
Benzene/Heptane (v/v = 3/2)	**G**	0.7
Toluene/Hexane (v/v = 2/1)	**G**	0.8
Toluene/Cyclohexane (v/v = 3/2)	**G**	0.9
Toluene/Heptane (v/v = 3/2)	**G**	0.5
Xylene/Hexane (v/v = 2/1)	**G**	0.8
Xylene/Heptane (v/v = 2/1)	**G**	1.0
Xylene/Cyclohexane (v/v = 3/2)	**PG**	
Dichloromethane	**S**	
Chloroform	**S**	
acetonitrile	**I**	
ethanol	**I**	
THF	**S**	
DMF	**S**	
DMSO	**S**	

[a] **G**: gel; **PG**: partial gelation at room temperature; **S**: soluble; **I**: insoluble.

[b] CGC is the minimum concentration required for the formation of a stable gel at room temperature.

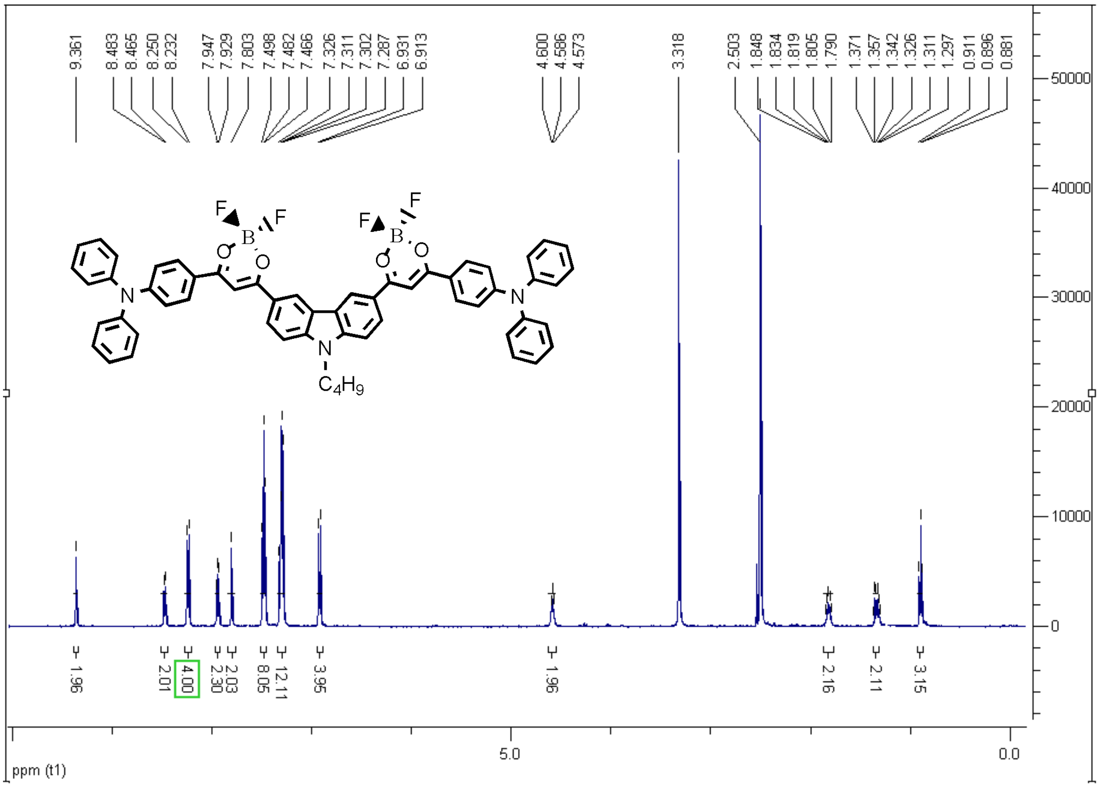

Fig. S1 [1]H NMR (500 MHz) spectrum of compound **BDOBC4**.

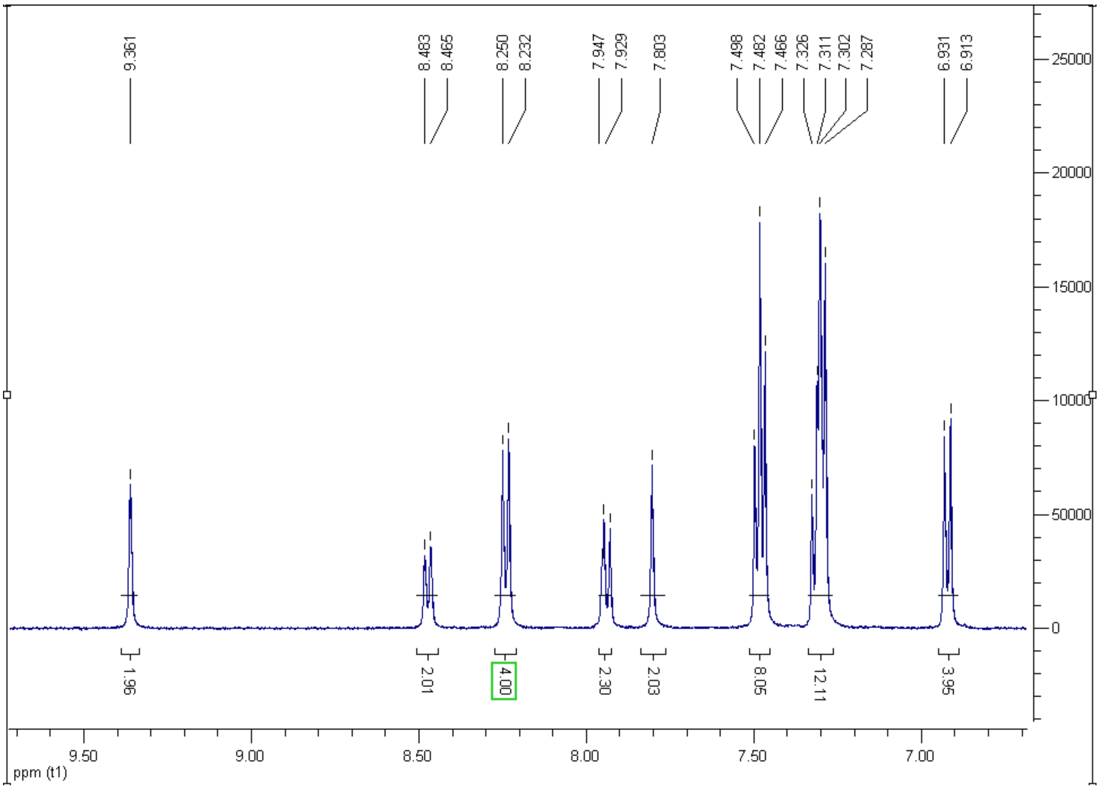

Fig. S2 [1]H NMR (500 MHz) spectrum of compound **BDOBC4**.

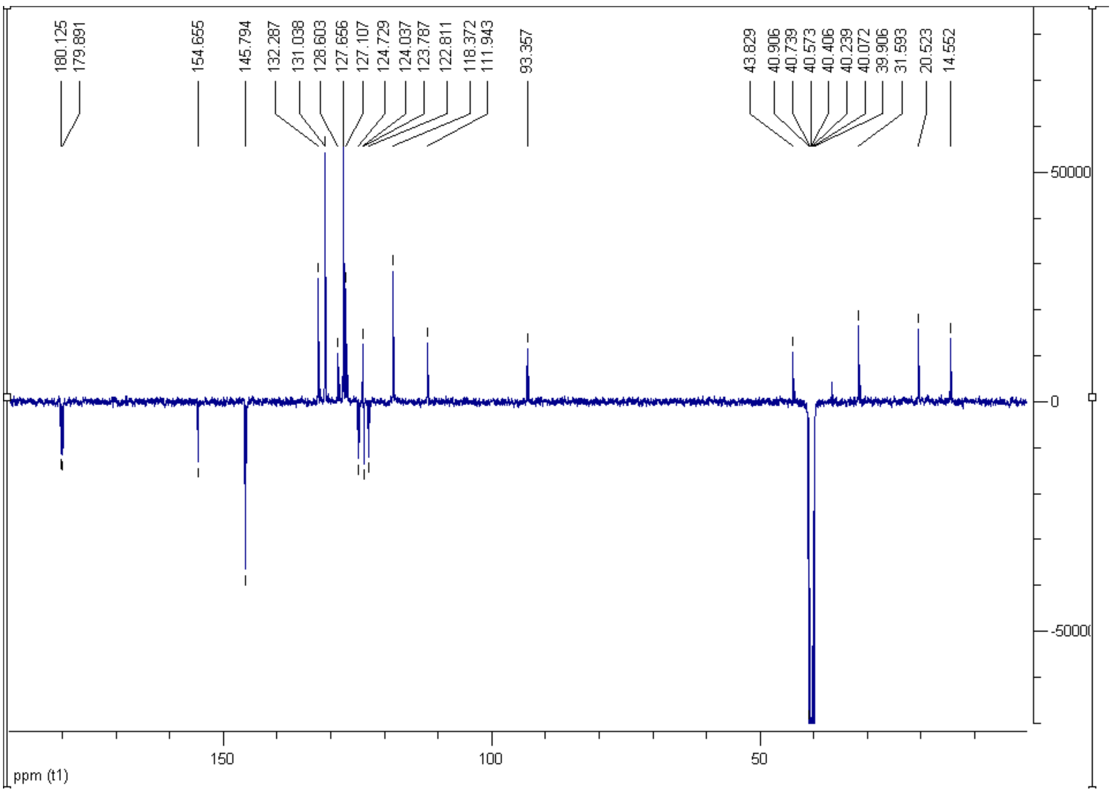

Fig. S3 ^{13}C NMR (125 MHz) spectrum of compound **BDOBC4**.

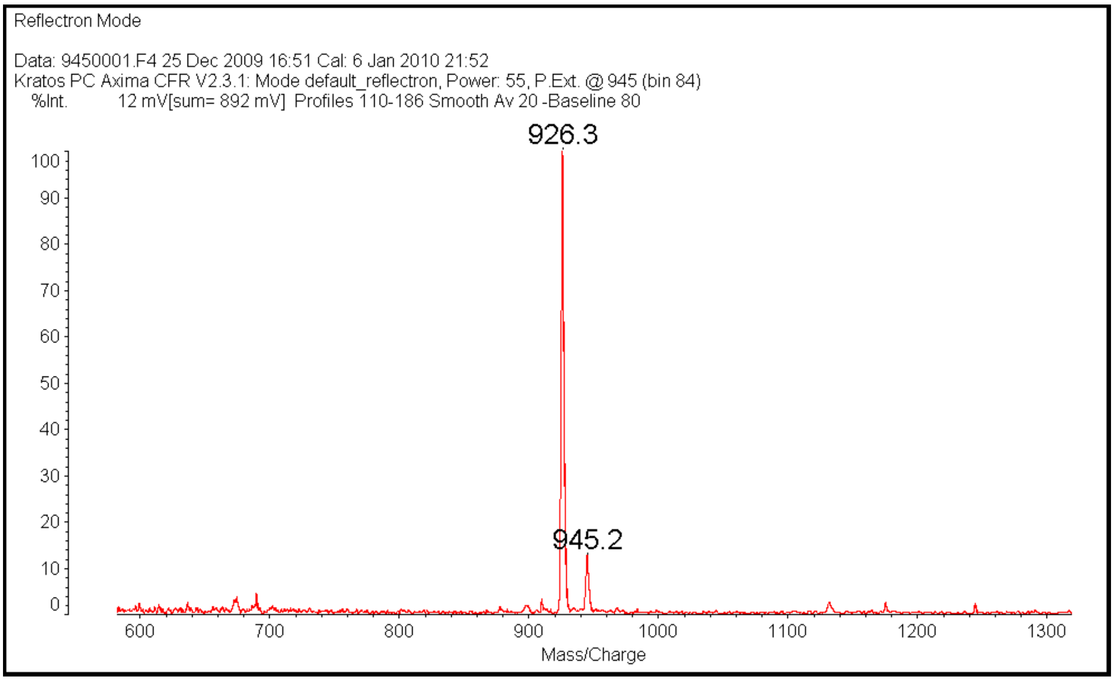

Fig. S4 MALDI/TOF MS spectrum of compound **BDOBC4**.

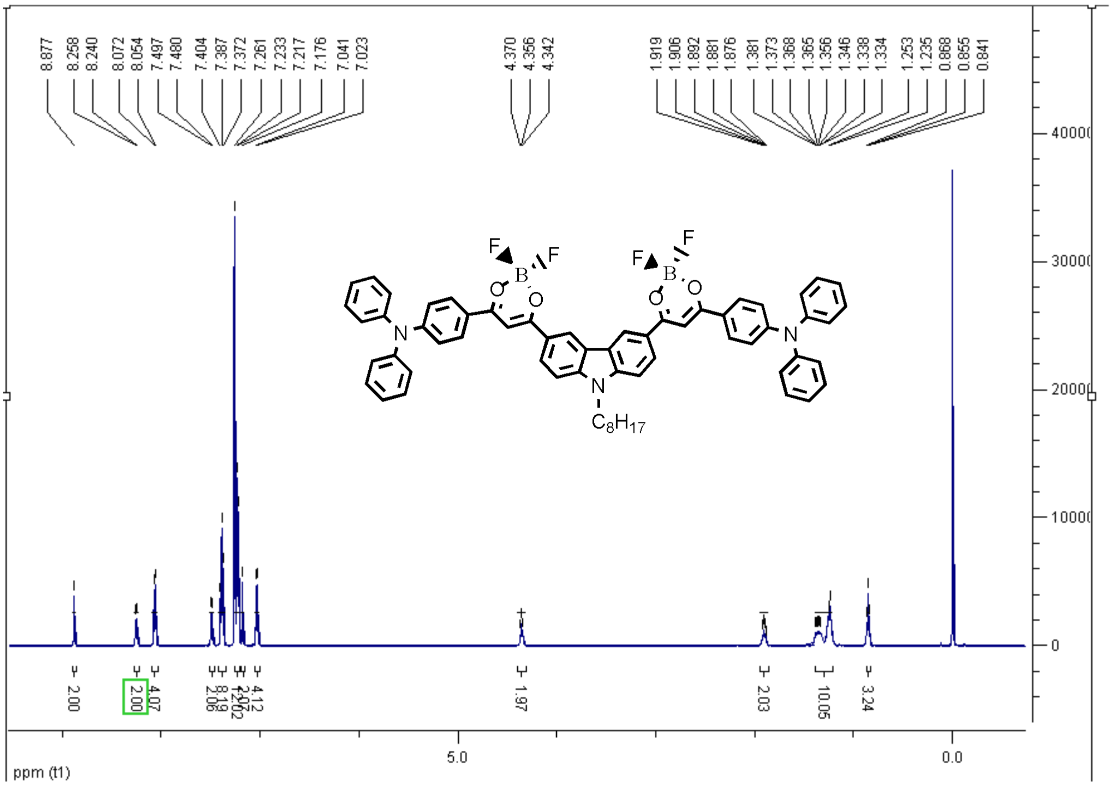

Fig. S5 ^{1}H NMR (500 MHz) spectrum of compound **BDOBC8**.

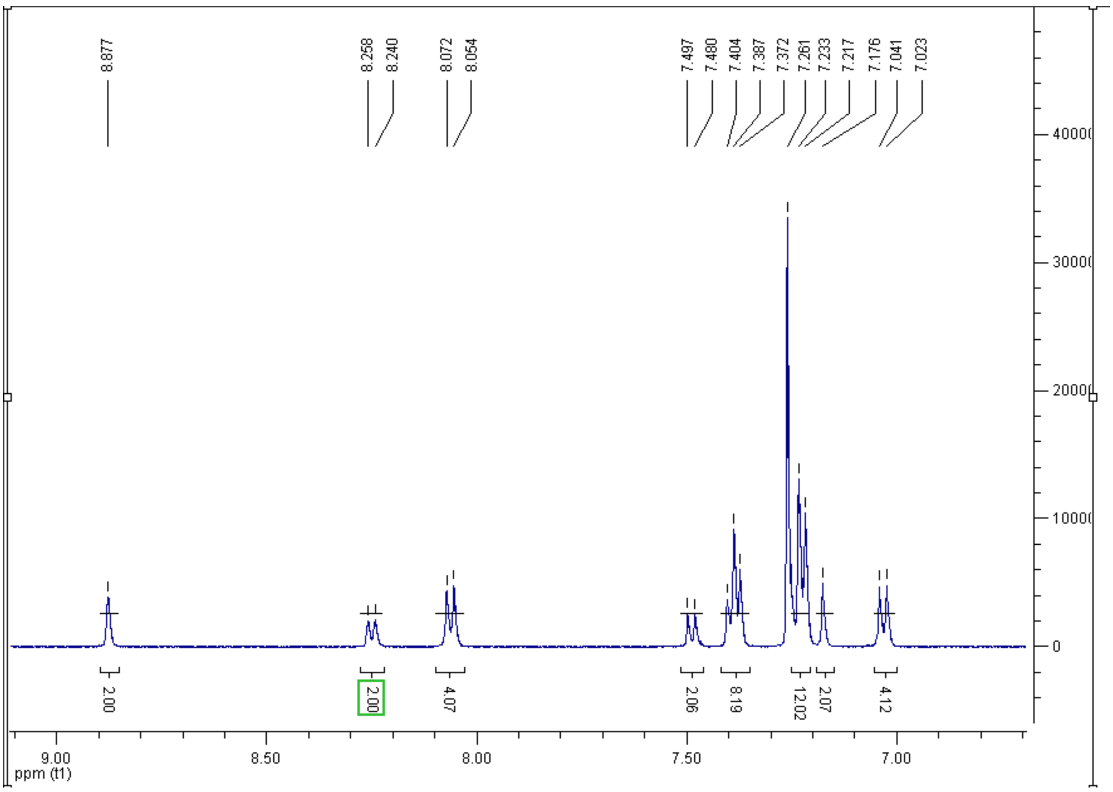

Fig. S6 ^{1}H NMR (500 MHz) spectrum of compound **BDOBC8**.

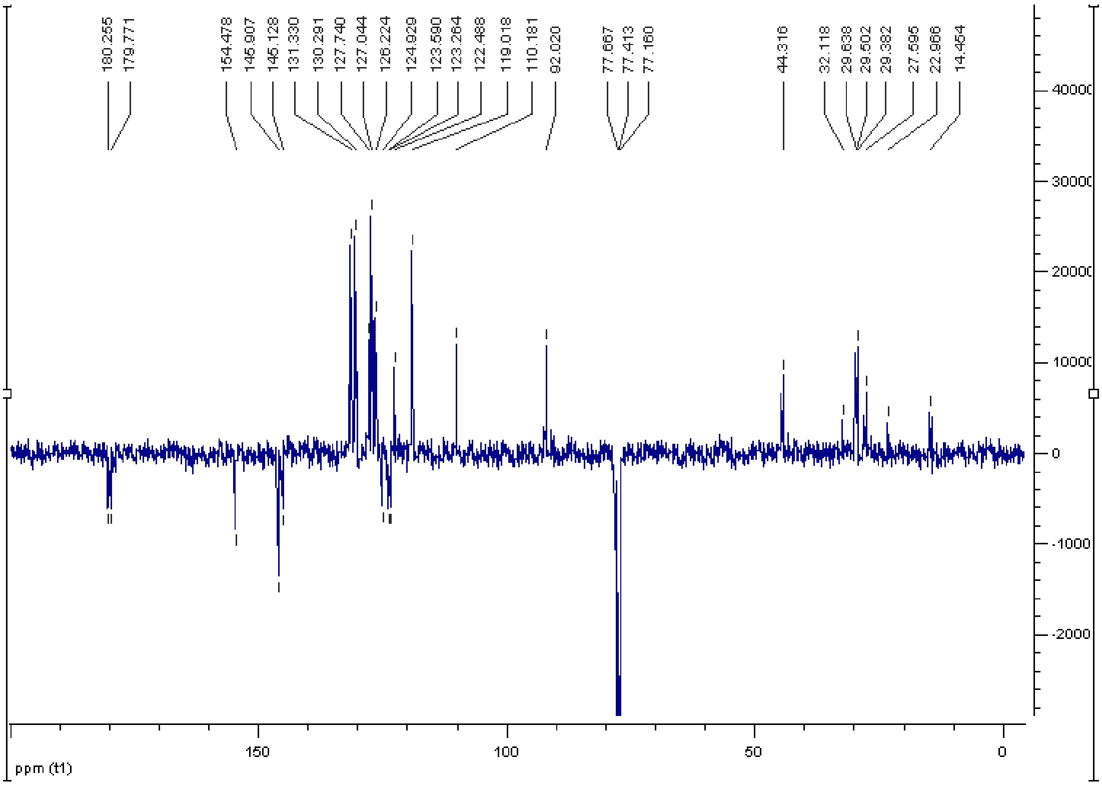

Fig. S7 [13]C NMR (125 MHz) spectrum of compound **BDOBC8**.

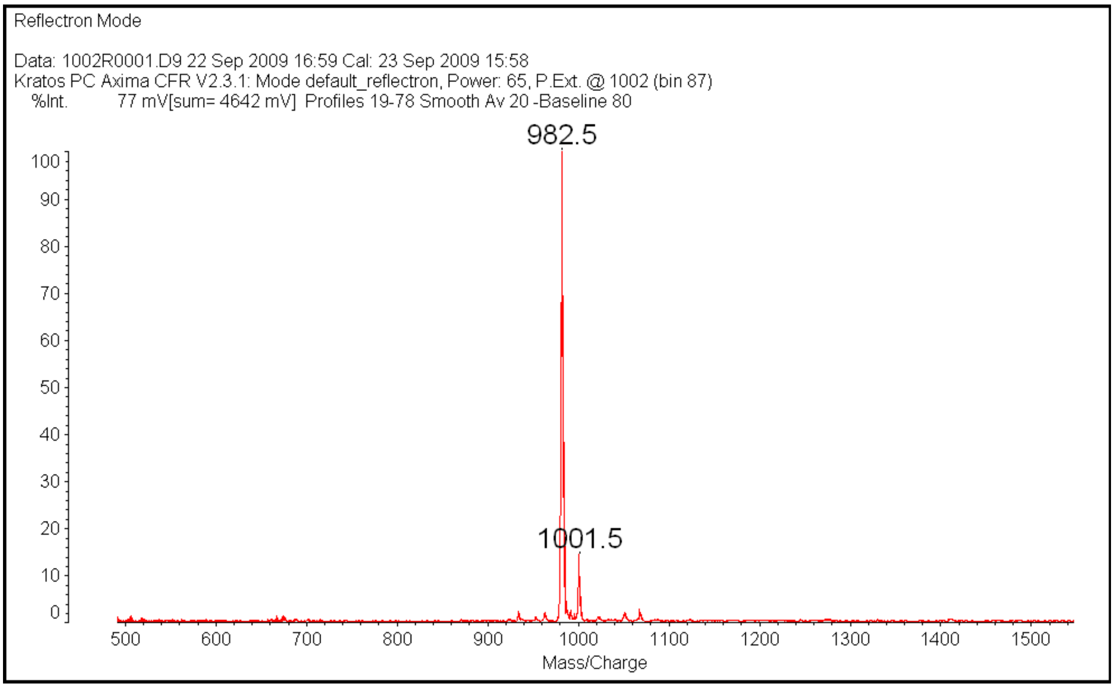

Fig. S8 MALDI/TOF MS spectrum of compound **BDOBC8**.

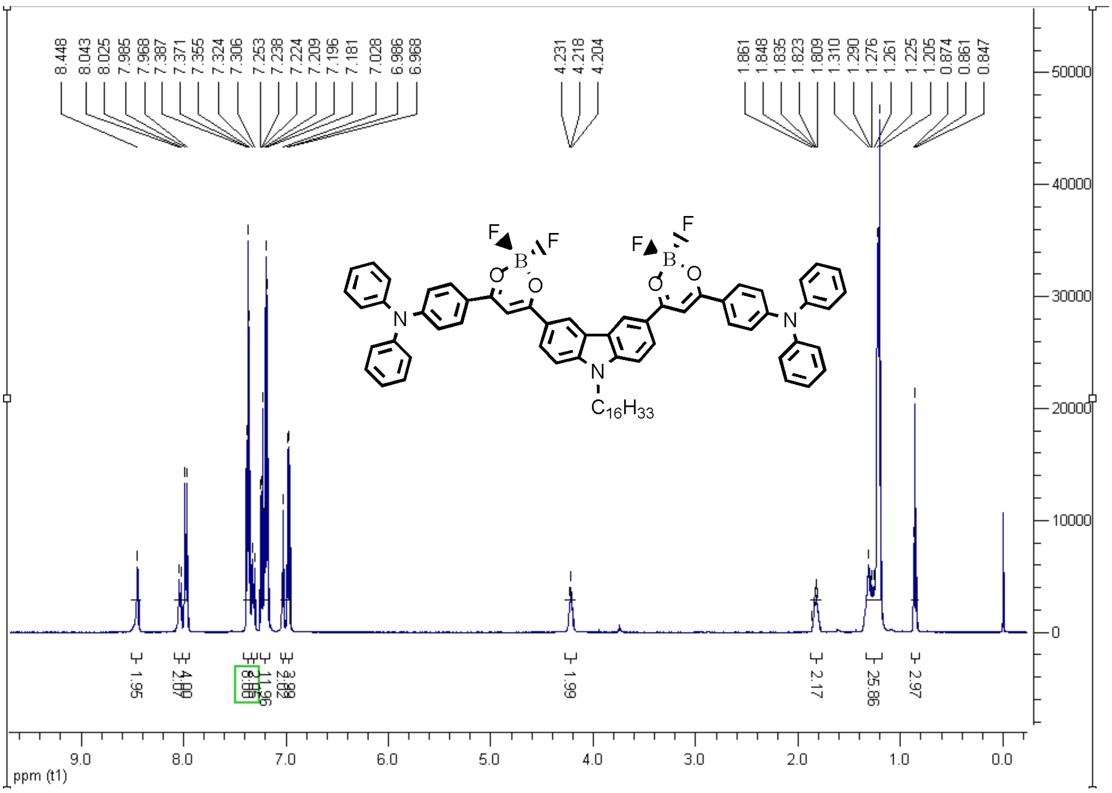

Fig. S9 ^{1}H NMR (500 MHz) spectrum of compound **BDOBC16**.

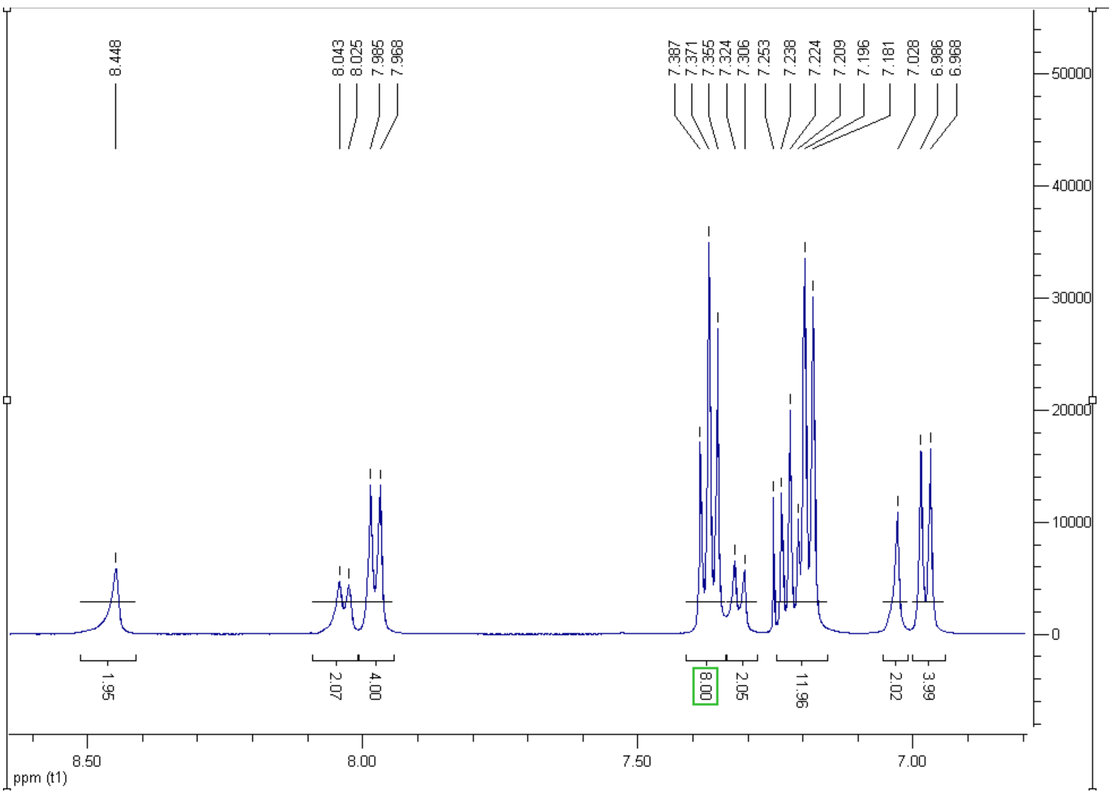

Fig. S10 ^{1}H NMR (500 MHz) spectrum of compound **BDOBC16**.

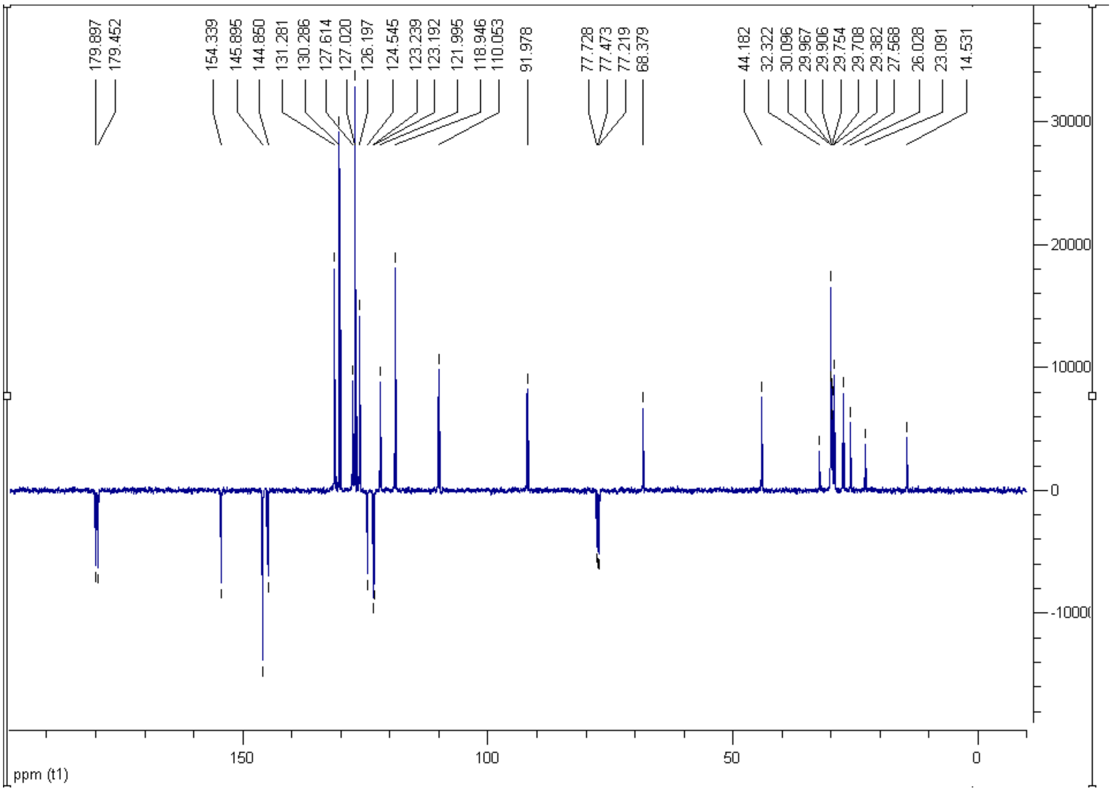

Fig. S11 ^{13}C NMR (125 MHz) spectrum of compound **BDOBC16**.

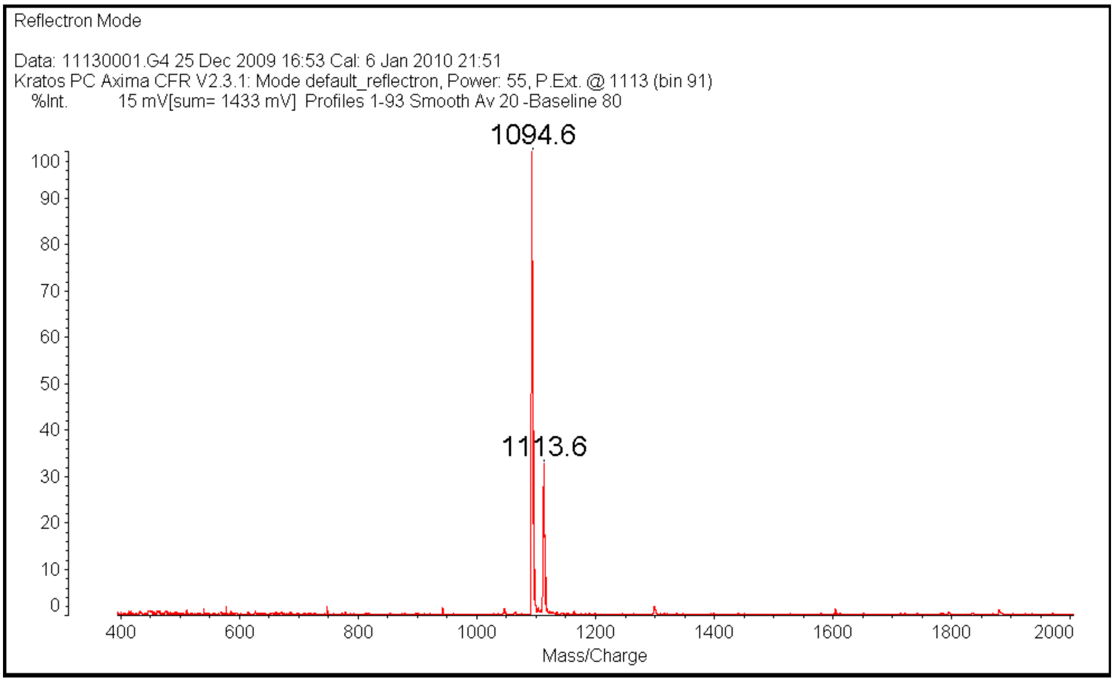

Fig. S12 MALDI/TOF MS spectrum of compound **BDOBC16**.

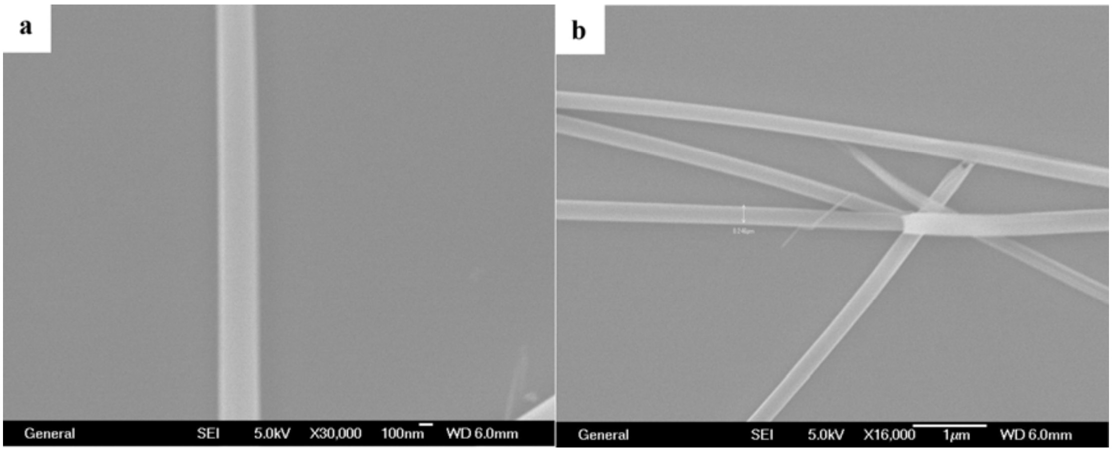

Fig. S13 SEM images of the nanowires based on **BDOBC4**.

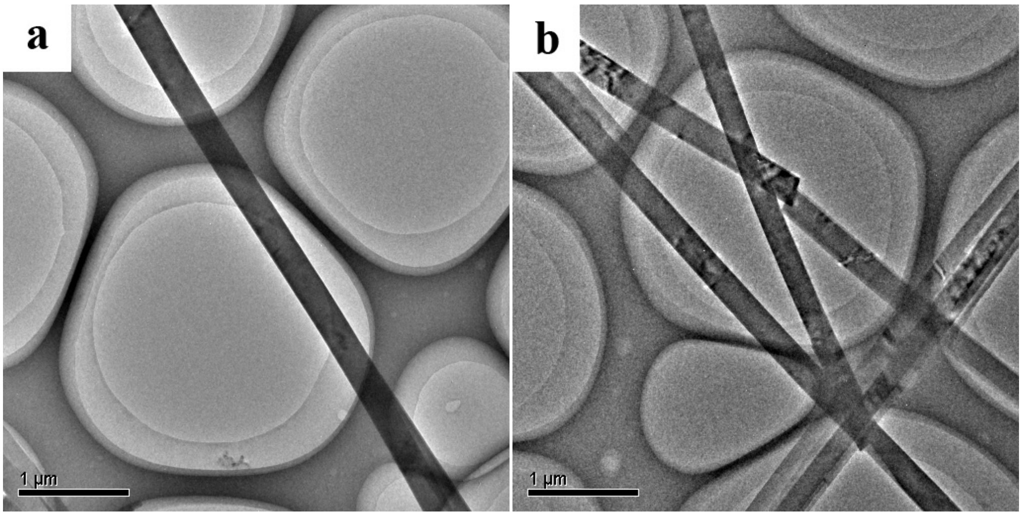

Fig. S14 TEM image of the nanwires based on **BDOBC4**, the broken nanowire in (b) demonstrates the belt-like geometry of the cross-section.

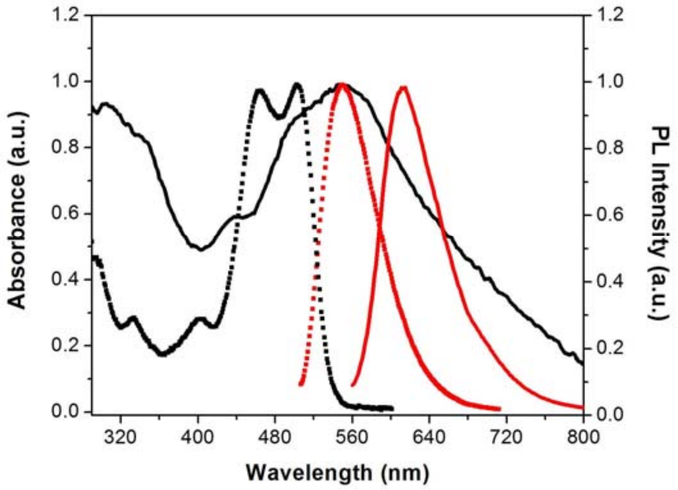

Fig. S15 The normalized UV/Vis absorption (black) and fluorescence (red, λ_{ex} = 504 nm) spectra of **BDOBC4** in toluene (1×10^{-6} M, dashed) and the nanowires based on **BDOBC4** deposited on quartz slide (solid). The raised baseline for the absorption spectrum of nanowires is primarily due to the light scattering.

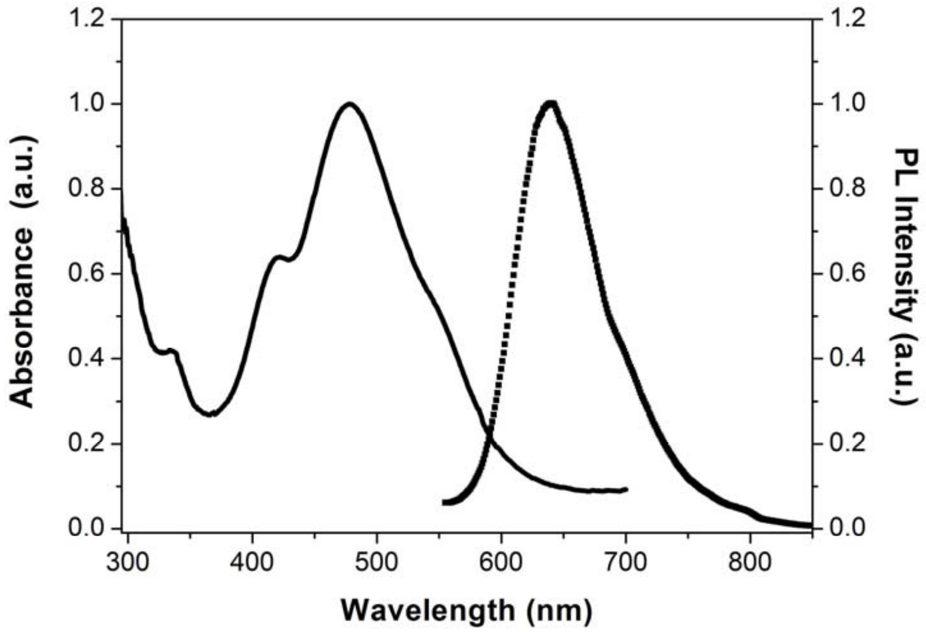

Fig. S16 The normalized UV/Vis absorption (solid) and fluorescence (dashed, λ_{ex} = 478 nm) spectra of the xerogel film based on **BDOBC16**.

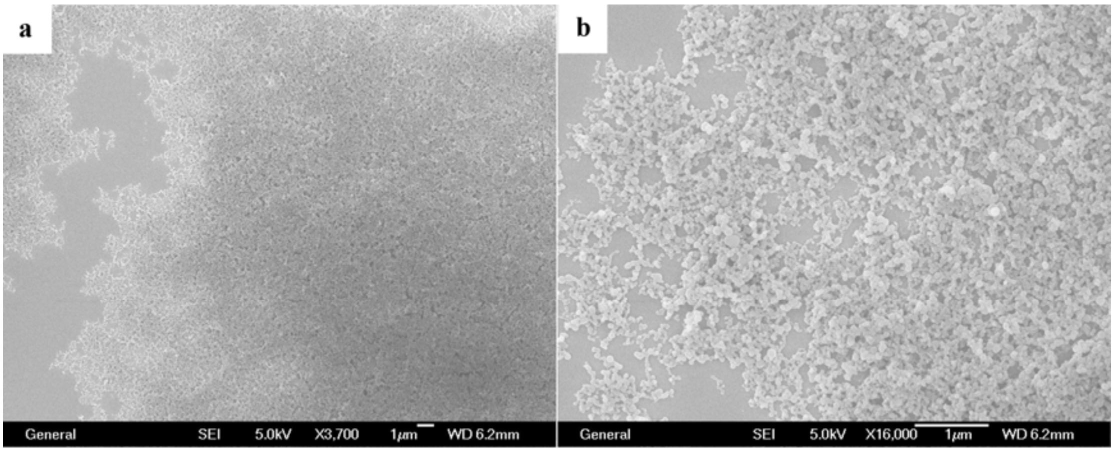

Fig. S17 SEM images of the nanoparticles based on **BDOBC8** on silicon wafer.

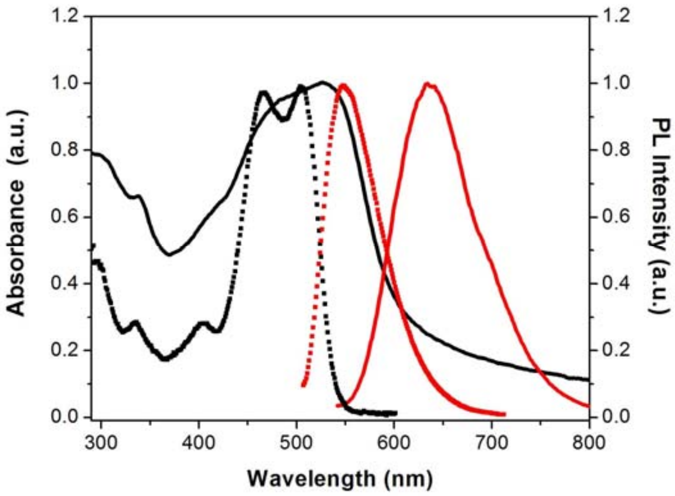

Fig. S18 The normalized UV/Vis absorption (black) and fluorescence (red, λ_{ex} = 504 nm) spectra of **BDOBC8** in toluene (1×10^{-6} M, dashed) and the nanoparticles based on **BDOBC8** deposited on quartz slide (solid).

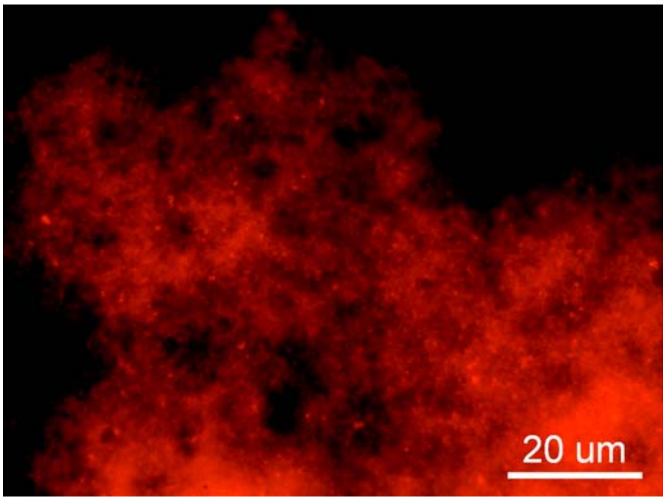

Fig. S19 Fluorescence microscopy image of **BDOBC8**-based nanoparticles obtained by reprecipitation approach (λ_{ex} = 510-550 nm).

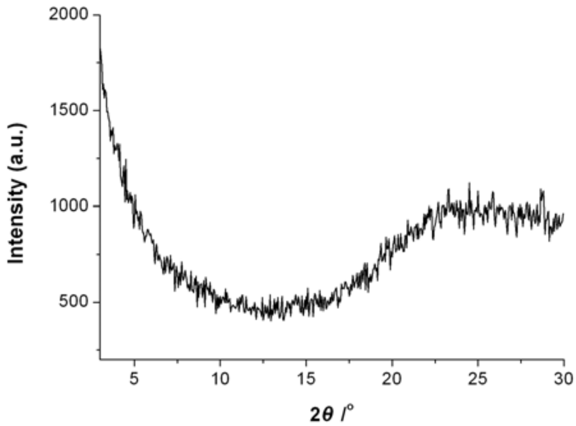

Fig. S20 X-ray diffraction pattern of the nanoparticles based on **BDOBC8** deposited on glass.

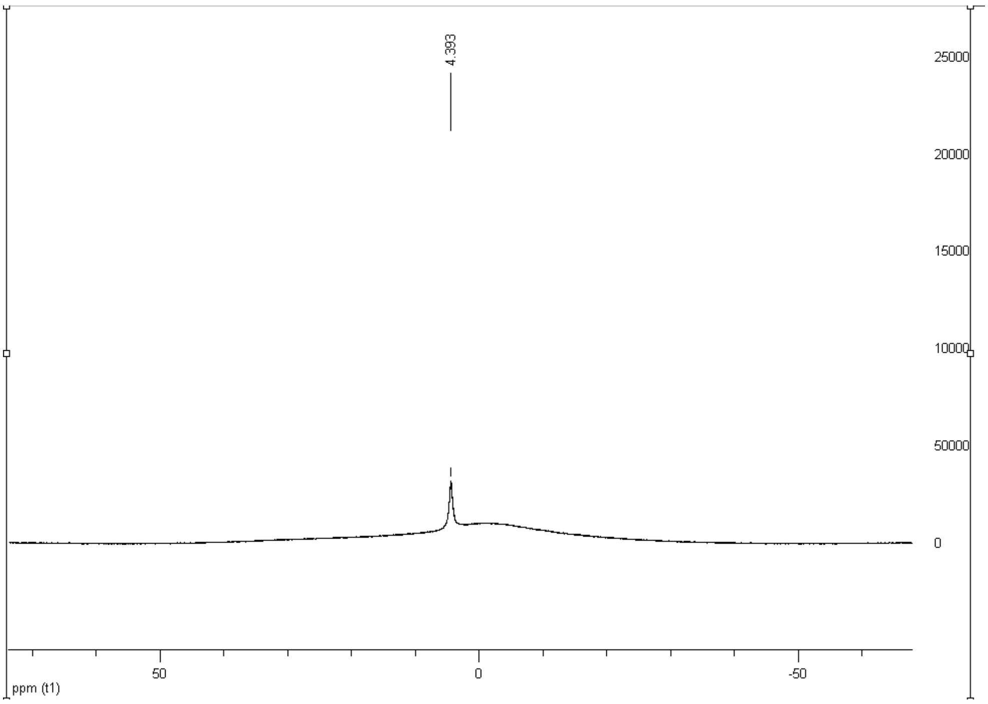

Fig. S21 ^{11}B NMR (160.4 MHz) spectrum of compound **BDOBC16**.

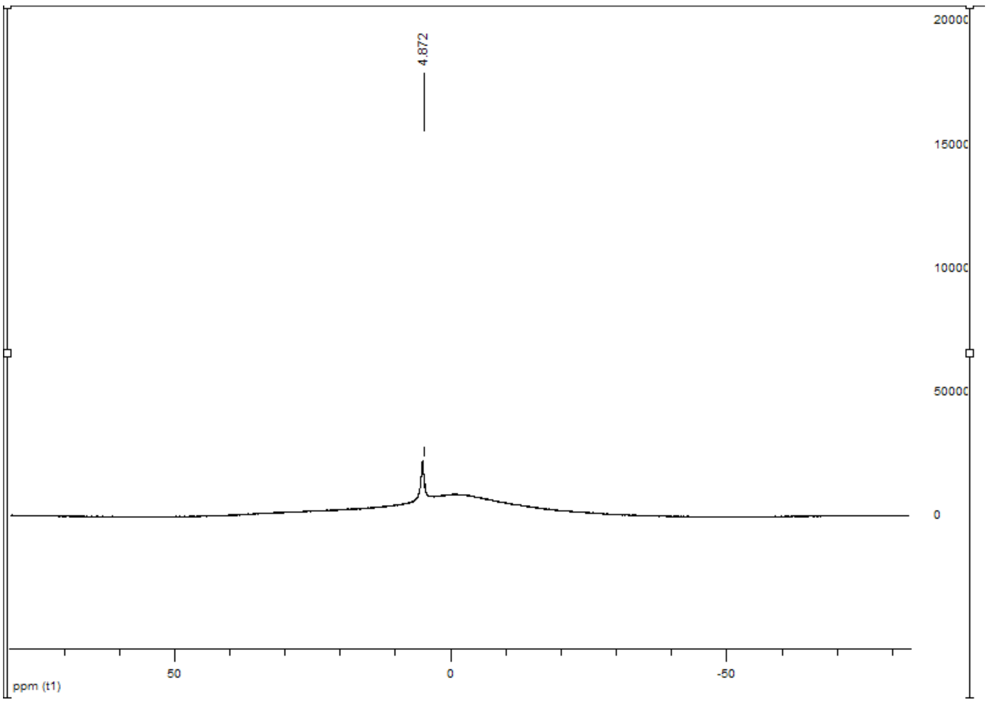

Fig. S22 ^{11}B NMR (160.4 MHz) spectrum of compound **BDOBC16** after adding aniline.

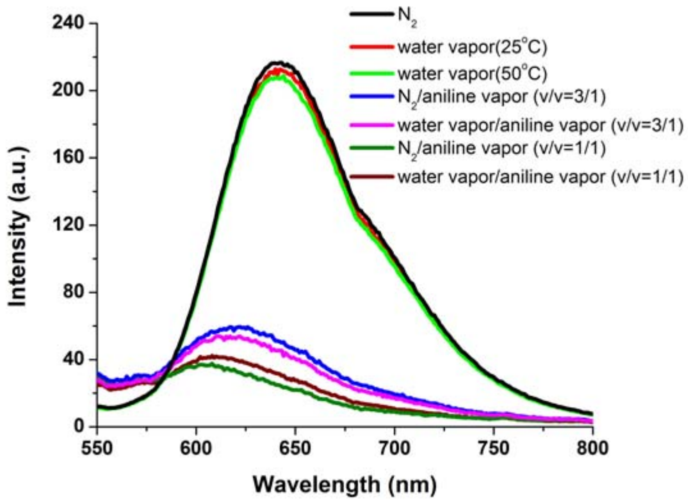

Fig. S23 Fluorescence response of the nanofiber-based film from **BDOBC16** upon exposure to the different vapors for 10 s.

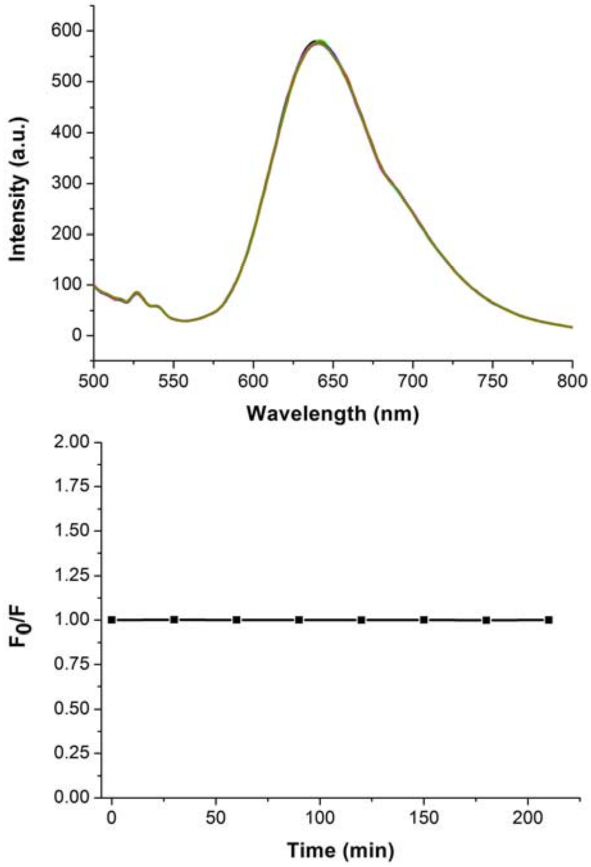

Fig. S24 Time-dependent fluorescence spectra (top, λex = 640 nm) and the plot of the ratio of fluorescent intensity at 640 nm (down) before and after exposing the nanofiber-based film from **BDOBC16** to air with the interval of 30 min at room temperature.

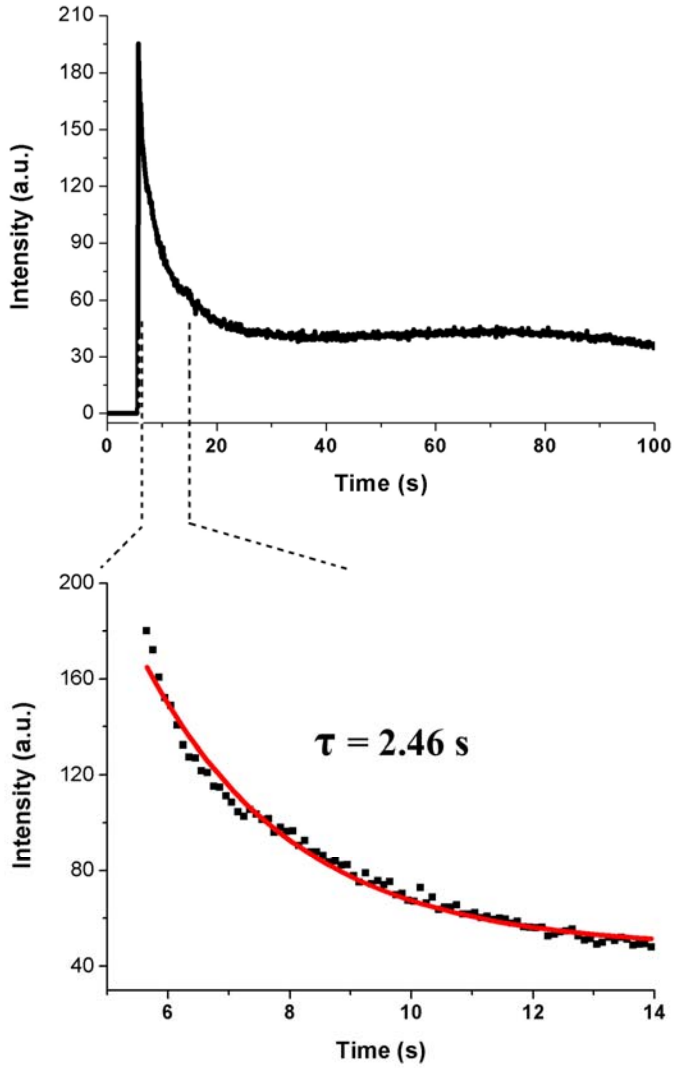

Fig. S25 Time-course of fluorescence quenching of the nanoparticle-based film from **BDOBC8** after been added into the cell filled with saturated vapor of aniline (880 ppm), indicating a response time of about 2.46 s. The intensity was monitored at 635 nm.

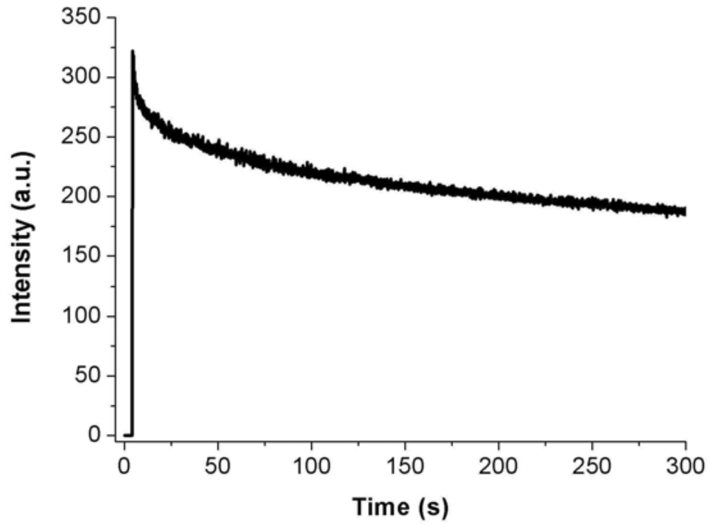

Fig. S26 Time-course of fluorescence quenching of a nanowire-based film of **BDOBC4** after been added into the cell filled with saturated vapor of aniline (880 ppm). The intensity was monitored at 613 nm.

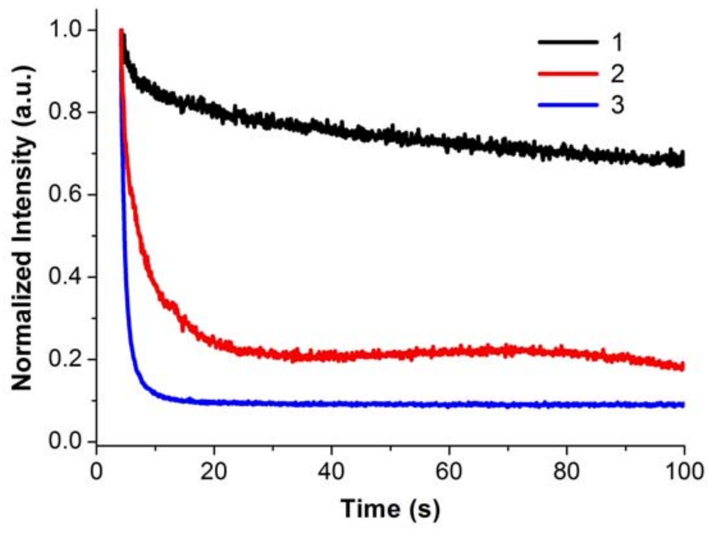

Fig. S27 Normilized time-course of fluorescence quenching of the films after been added into the cell filled with saturated vapor of aniline (880 ppm): 1) nanowire-based film of **BDOBC4**; 2) nanoparticle-based film of **BDOBC8**; 3) gel nanofiber-based film of **BDOBC16**. The intensity was monitored at 613, 635 and 640 nm, respectively.